

## Lateral IBIC Analysis of Diamond Detectors

A. Lo Giudice<sup>1</sup>, L. La Torre<sup>2</sup>, C. Manfredotti<sup>1</sup>, M. Marinelli<sup>3</sup>, P. Olivero<sup>1</sup>, F. Picollo<sup>1</sup>, A. Re<sup>1</sup>, V. Rigato<sup>2</sup>, E. Vittone<sup>1</sup>.

<sup>1</sup>Experimental Physics Department- NIS Excellence Centre, University of Torino and INFN-sez. Torino, Italy.

<sup>2</sup>INFN, Laboratori Nazionali di Legnaro, Legnaro (Padova), Italy.

<sup>3</sup>Dipartimento di Ingegneria Meccanica, University of Roma "Tor Vergata", Roma, Italy.

### INTRODUCTION

In order to evaluate the charge collection efficiency (CCE) profile of a single-crystal diamond devices based on a p type/intrinsic/metal configuration, a lateral Ion Beam Induced Charge (IBIC) analysis was performed over its cleaved cross section using a 2 MeV proton microbeam. CCE profiles in the depth direction were extracted from the cross-sectional maps at variable bias voltage. IBIC spectra relevant to the depletion region extending beneath the frontal Schottky electrode show a 100% CCE, with a spectral resolution of about 1.5%. The dependence of the width of the high efficiency region from applied bias voltage allows the constant residual doping concentration of the active region to be evaluated. The region where the electric field is absent shows an exponentially decreasing CCE profile, from which it is possible to estimate the diffusion length of the minority carriers by means of a drift-diffusion model.

### EXPERIMENTAL

The device was developed starting from a single-crystal diamond grown by CVD technique at the laboratories of Rome "Tor Vergata" University. Diamond was grown on a HPHT substrate in a p-type/intrinsic layered structure by a two-step plasma-enhanced microwave CVD homoepitaxial deposition process. A cross-sectional schematic of the device is reported in figure 1 [1]. The sample was cleaved in order to expose the cross section to the ion beam irradiation and edge-on mounted to perform lateral IBIC experiments.

IBIC measurements were carried out at the AN2000 microbeam facility by using 2 MeV protons.

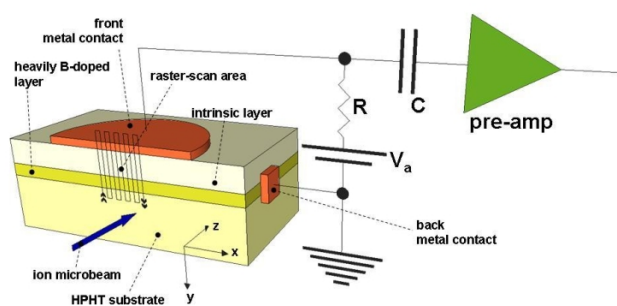


Fig. 1. Schematic of the diamond detector cross-sectional structure, connection to the acquisition electronic chain, and ion beam probe geometry. The drawing is not to scale.

The beam was focused to a spot size of  $\sim 2 \mu\text{m}$  and raster-scanned over the cleaved cross section of the diamond sample from the Schottky contact to the highly doped substrate ( $62 \times 62 \mu\text{m}^2$  scan area), as schematically shown in figure 1.

As evaluated by the SRIM Monte Carlo Simulation code [2], the range of 2 MeV protons in diamond is about  $25 \mu\text{m}$ , while their lateral straggling is  $\sim 0.66 \mu\text{m}$ . Since the electron/hole generation occurs primarily at the Bragg's peak, it is reasonable to assume negligible charge or recombination effects at the irradiated cross-section surface.

The system provided a spectral sensitivity of 270 electrons/channel and a spectral resolution (defined as the FWHM of the 2 MeV proton peak in the Si surface-barrier detector used as reference) of about 3900 electrons, corresponding to an energy resolution of 14 keV in silicon

### RESULTS AND DISCUSSION

Figure 2 shows lateral IBIC maps at different reverse bias voltages. The CCE is encoded in colour scale, being derived from the median of the IBIC pulse distribution for each pixel.

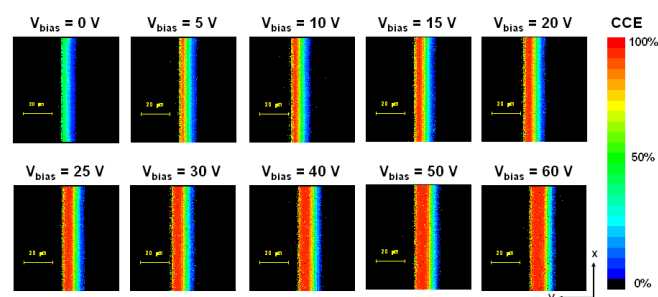


Fig. 2. Lateral IBIC maps relevant to bias voltages from 0 Volt to 60 V. The Schottky frontal sensitive electrode is on the left and the B doped back electrode is on the right.

The highest charge is induced by the motion of carriers generated in the proximity of the Schottky electrode, which roughly corresponds to the depletion region where a strong electric field occurs. At zero bias, the maximum induced charge occurs in a region extending around  $5 \mu\text{m}$  beneath the Schottky barrier; as the applied bias increases, the extension of the high efficiency IBIC region widens.

In figure 3 the CCE profiles obtained by projecting the CCE maps along the y axis are reported.

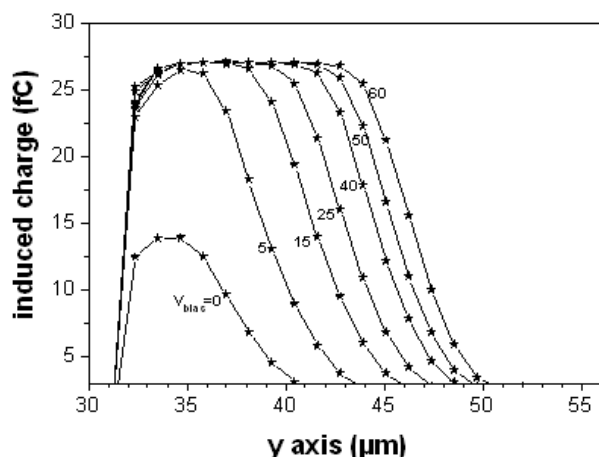


Fig. 3. CCE profiles at different bias voltages.

These profiles exhibit the same behaviour observed in previously analyzed partially depleted silicon p-n junctions [3] and Schottky diodes [4], which have been interpreted using the drift-diffusion model for charge induction based on the Shockley-Ramo-Gunn theorem [5]. The dependence of the extension of the depletion region  $W$  from the applied voltage  $V_a$  can be interpolated with the well known formula:

$$W = \sqrt{2 \cdot \varepsilon_r \cdot \varepsilon_0 \cdot (V_a + V_{bi}) / (e \cdot N_A)} \quad (1)$$

where  $\varepsilon_r$  and  $\varepsilon_0$  are the relative and vacuum dielectric constants,  $e$  is the elementary electrical charge,  $N_A$  is the net electrically active acceptor-like defect concentration and  $V_{bi}$  is the built-in potential at the Schottky barrier.

As shown in figure 4, the experimental data are satisfactorily fitted by this trend, yielding a value of the built in voltage of  $(1.3 \pm 0.8)$  V and an estimation of the net electrically active acceptor-like defect concentration of  $N_a = (2.43 \pm 0.13) \cdot 10^{14} \text{ cm}^{-3}$ , in good agreement with previous estimations [1].

The fit procedure of the exponentially decreasing tails reported in Fig. 3 provides an average electron diffusion length of  $L_e = (2.6 \pm 0.2) \mu\text{m}$ , in excellent agreement with the value reported in [1]. Using the Einstein relation for the diffusivity/mobility ratio, the product of the zero field mobility ( $\mu_e$ ) and the lifetime is evaluated as  $\mu_e \cdot \tau_e = (2.5 \pm 0.3) \cdot 10^{-6} \text{ V cm}^{-2}$ , a value which is in good agreement with what reported in [6,7], providing an electron lifetime estimate of  $\sim 1$  ns, if a mobility of the order of  $2000 \text{ cm}^2 \text{ V}^{-1} \text{ s}^{-1}$  is considered [8,9].

### CONCLUSIONS

Lateral IBIC characterization was employed to characterize the charge transport properties of SC diamond devices. In the active region, the device yielded a 100% efficiency with a spectral resolution of about 35 keV.

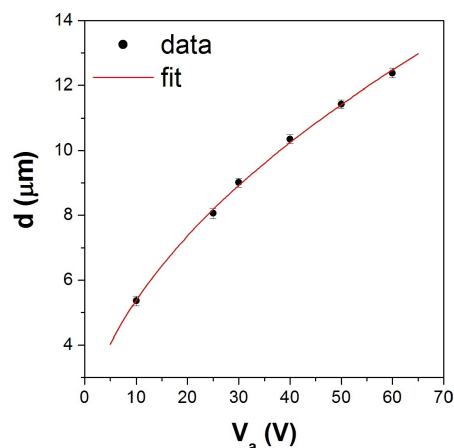


Fig. 4. Plot of the extension of the depletion region as evaluated from the IBIC maps as a function of applied bias voltage.

The variation of the width of the depletion region as function of the applied bias voltage allows the estimation of the acceptor-like defect concentration in the nominally intrinsic layer to a value of  $(2.43 \pm 0.13) \cdot 10^{14} \text{ cm}^{-3}$ . The analysis of the tails of the CCE profiles provides a value of the mobility-lifetime product for electrons of  $2.5 \cdot 10^{-6} \text{ cm}^2 \text{ V}^{-1}$ , which corresponds to an average lifetime of the order of  $\sim 1$  ns if typical mobility values are assumed.

### ACKNOWLEDGMENTS

This work was supported in the framework of the INFN experiment DIARAD and MiUR-PRIN2008 National Project “Synthetic single crystal diamond dosimeters for application in clinical radiotherapy”. The work of P. Olivero was supported by the “Accademia Nazionale dei Lincei – Compagnia di San Paolo” Nanotechnology grant.

- 
- [1] S. Almviva et al., *J. Appl. Phys.*, 107 (2010) 014511.
  - [2] J. F. Ziegler, J. P. Biersack, M. D. Ziegler, “SRIM – The Stopping and Range of Ions in Matter”, Ion Implantation Press, 2008.
  - [3] C. Manfredotti et al., *Nucl. Instr. and Meth. B*, 158 (1999) 476.
  - [4] P. Olivero et al., *Nucl. Instr. and Meth. B*, in press, DOI: 10.1016/j.nimb.2011.02.020.
  - [5] M. B. H. Breese et al., *Nucl. Instr. and Meth. B*, 264 (2007) 345.
  - [6] J. Isberg et al., *Diamond Relat. Mater.*, 13 (2004) 872.
  - [7] A. Lohstroh et al., *Appl. Phys. Lett.*, 90 (2007) 102111.
  - [8] L.S. Pan and D.R. Kania, *Diamond: Electronic Properties and Applications*, Kluwer Academic Publishers, Boston - Dordrecht - London, 1993.
  - [9] M. Marinelli et al., *Appl. Phys. Lett.*, 89 (2006) 143509.